Electrochemical Synthesis of the *in human S*-oxide metabolites of phenothiazine containing Anti-Psychotic Medications

Ridho Asra[1], Aigul Erbosynovna Malmakova[1,2], and Alan M. Jones[1*]

[1]School of Pharmacy, Institute of Clinical Sciences, College of Medical and Dental Sciences, University of Birmingham

[2] Bekturov Institute of Chemical Sciences, Almaty, 050010, Kazakhstan

* Corresponding author: Dr Alan M. Jones; +44(0)121-414-7288; a.m.jones.2@bham.ac.uk

Abstract

The tractable preparation of phase-I drug metabolites is a critical step to understand the first-pass behaviour of novel chemical entities in drug discovery. In this study we have developed a structure electroactivity relationship (SeAR) informed electrochemical reaction of the parent 2-chlorophenothiazine and anti-psychotic, chlorpromazine. The ability to dial-in under current controlled conditions the formation of *S*-oxide and novel *S,S*-dioxide metabolites has been achieved for the first time on a multimilligram scale using a direct batch electrode platform. A potential rationale for the electrochemical formation of these metabolites *in situ* is proposed using molecular docking to a cytochrome P_{450} enzyme.

Keywords

Electrochemistry, metabolite, phenothiazine, chlorpromazine.

Introduction

Phenothiazine (PTZ) is a heterocyclic pharmaceutical lead structure in medicinal chemistry,[1] representing a major class of antipsychotic drugs that have an inhibitory effect against dopaminergic receptors, especially D_2 receptor.[2] Derivatives of PTZ have been extensively used to treat psychosis, including schizophrenia, violent, agitated, disturbed behaviour and bipolar disorder.[3] While these medications are effective, side effects of PTZs include 1) the autonomic and cardiovascular systems, endocrinologic, metabolic, hematologic, hepatic, allergic/dermatologic, ophthalmologic, and anticholinergic effects; 2) the central nervous system, including extrapyramidal symptoms, tardive dyskinesia, neuroleptic malignant syndrome, seizure, and sedation; 3) the sexual and reproductive side effects, including sexual dysfunction, and teratogenicity.[4] These side effects are primarily caused by the PTZs' non-selective blocking of receptors in the central nervous system, including dopamine (D_1 and D_2), muscarinic, histamine H_1, and serotonergic 5-hydroxytryptamine (HT) 2 receptors.[5] Clinical studies have shown that these side effects occur due to bioactive metabolites, which may significantly contribute to the toxicity in humans.[6] Sulfoxide metabolites has been annotated to be responsible for cardiotoxic activity,[7] and 7-hydroxylated metabolite of the PTZs, form an electrophilic quinone imine intermediate, which is responsible for mechanisms of drug-induced idiosyncratic hepatotoxicity.[8] PTZ analogues are classified into three groups, as shown in **Table 1**.[1][9]

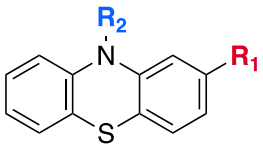

Type of Compound	Example	Activity	R_1	R_2
Lead Structure	Phenothiazine (PTZ)	anthelmintic	H	**H**
(1) Aminoalkyl compound	2-Chlorophenothiazine (2CPTZ)	sedatives and antipsychotic	-Cl	H
	Chlorpromazine (CPZ)	antipsychotic		
	Promethazine	antihistamine	H	
(2) Piperidine	Thioridazine	antipsychotic	$-SCH_3$	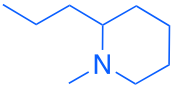
(3) Piperazine	Trifluoperazine	antipsychotic	$-CF_3$	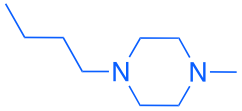
	Fluphenazine	antipsychotic		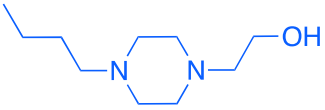

Table 1. PTZ structure and their respective classifications (1-3) and bioactivities.

2-Chlorophenothiazine (2CPTZ), is an important intermediate in the synthesis of neuroleptic drugs, such as chlorpromazine (CPZ), perphenazine, prochlorperazine.[10] CPZ is subject to a significant amount of first-pass metabolism, including hydroxylation, *N*-dealkylation, *N*-oxidation, and *S*-oxidation.[11-13] Chlorpromazine (CPZ) is primarily metabolized as chlorpromazine-*S*-oxide (CPZ-SO) and was found to have the same effect as CPZ in the vasomotor and central nervous systems. Chemical methods to oxidise PTZ derivatives to sulfoxide are shown in **Scheme 1**. Owens and co-workers prepared phenothiazine sulfoxide (PTZ-SO) using aqueous nitrous acid and hydrogen peroxide at room temperature (PTZs-SO, 95% yield with CPZ-SO, yield 74%).[14] Ryoji and co-workers investigated the preparation of sulfoxide compounds using aqueous hydrogen peroxide, a tungstate complex, and a quaternary ammonium hydrogensulfate as an acidic phase-transfer catalyst in 95% yield. [15] Bosch and colleagues also reported sulfoxidation using nitric oxide oxidation (CPZ-SO, 99% yield).[7] Liu and colleagues used ferric nitrate nonahydrate ($Fe(NO_3)_3.9H_2O$) as a catalyst and oxygen as a green oxidant for the selective oxidation from thioethers to sulfoxides including on CPZ with an 88% yield.[16] Stadler and Roth reported a microfluidic electrochemical preparation of CPZ-sulfoxide.[17] Four drugs were subjected to continuous-flow electrolysis, including the conversion of CPZ to CPZ-SO with an 83% isolated yield. However, this technique has some limitations, including 1) microfluidic-electrosynthesis can be complex to design, set up, and operate, 2) and high-cost equipment.

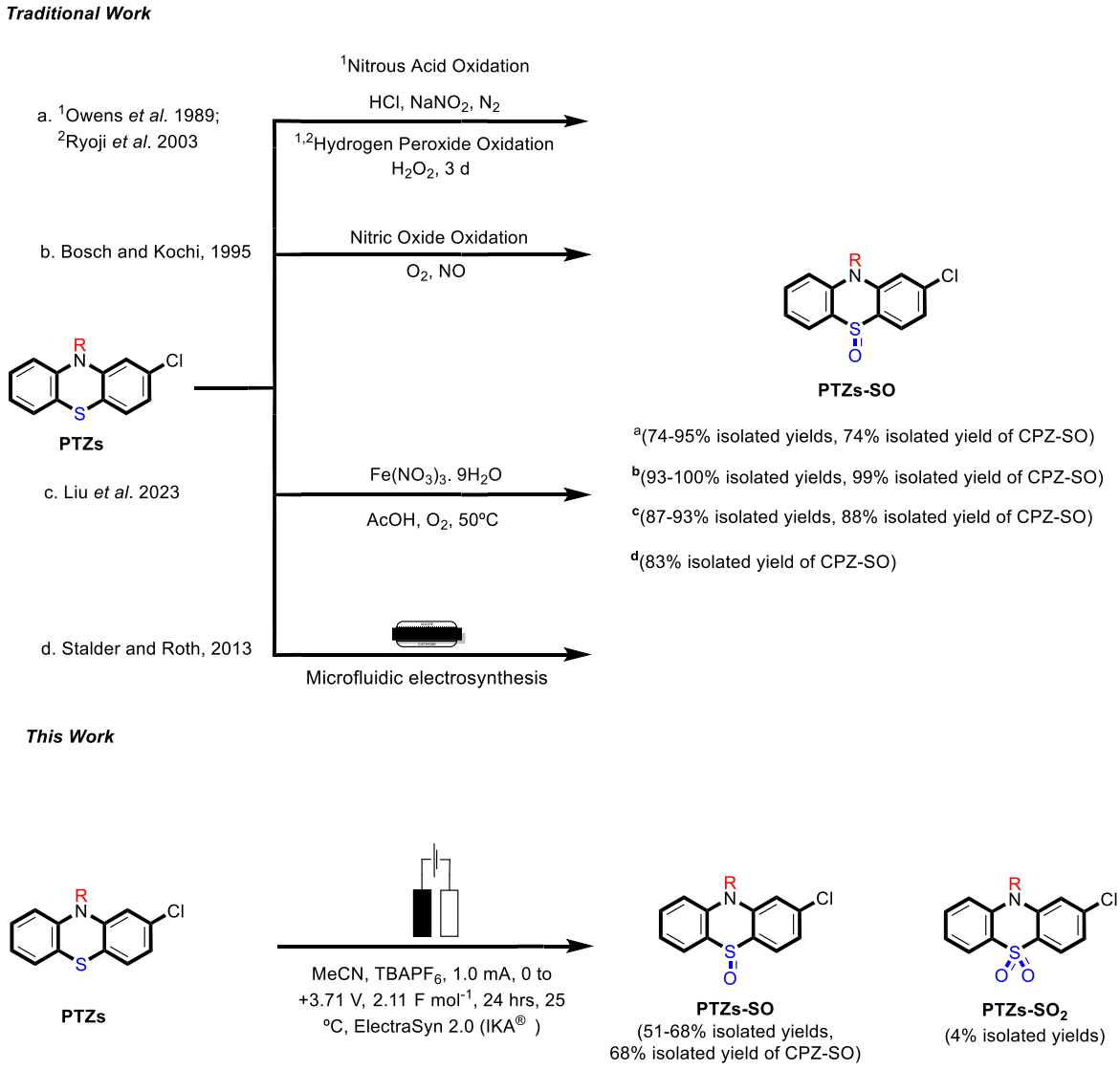

Scheme 1. Previous approaches (a-d) towards synthesising PTZs sulfoxide using chemical oxidants and microfluidic electrosynthesis and this study: a green electrosynthesis approach.

In this work, we explored electrochemistry a green technique [18] to determine the voltammetric behaviour [19] and patterns within PTZ analogues and generate the oxidation metabolites of 2-CPTZ and CPZ. [20-21]

Result and Discussion

To explore the structure electroactive relationships (SeAR) [22] between the PTZ analogues represented by 2-CPTZ and CPZ, we sought to develop a modular synthesis of R1 and R2 point variables during a related medchem campaign (**Scheme 2**).

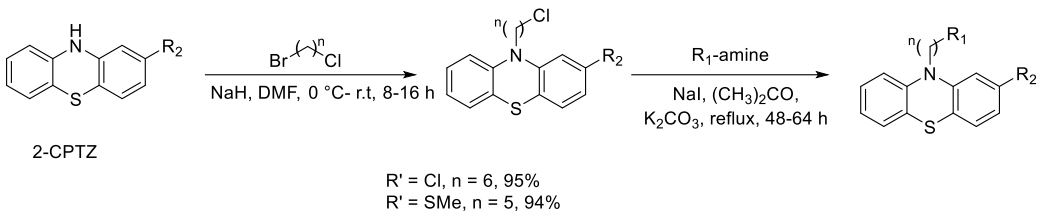

Structures	^{1}Ep (V)
2CPTZ	0.353
CPZ	0.590
1	0.513
2	0.437
3	0.598
4	0.484
5	0.478
6	0.459
7	0.469
8	0.430

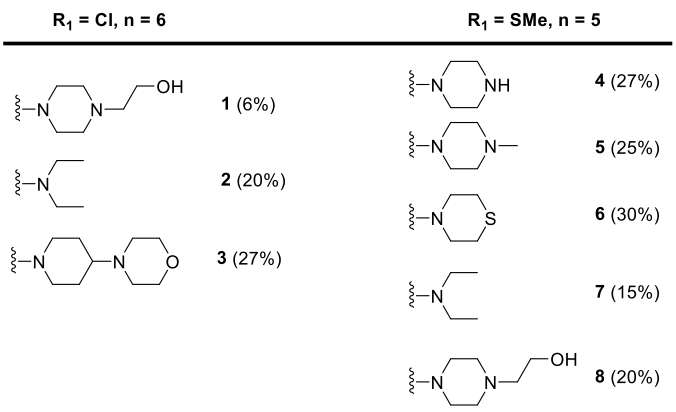

Scheme 2. General synthesis of novel PTZ containing structures to explore linker length and amine effect. Summary of initial oxidation potentials observed in PTZ analogues derived from cyclic voltammetry measurements.

With eight novel analogues, alongside 2CPTZ and CPZ, the cyclic voltammetric behaviour was determined (see supporting materials), a summary of the effect of functional group on oxidizability is shown in **Scheme 2.** Two clear SeAR trends emerged. The presence of a chlorine generally increased the difficulty with which the PTZ scaffold undergoes oxidation compared to an additional thiomethyl group. The ease of oxidisability of the free NH analogue (2CPTZ) versus all alkylated analogues explored (0.353 V vs 0.590V for CPZ). With this tentative SeAR in hand, initial optimisation studies for the electrosynthesis of metabolites commenced with the parent scaffold, 2CPTZ via enhanced CV studies.[23] To the best of our knowledge, no CV study of 2CPTZ has been reported (**Figure 2**).

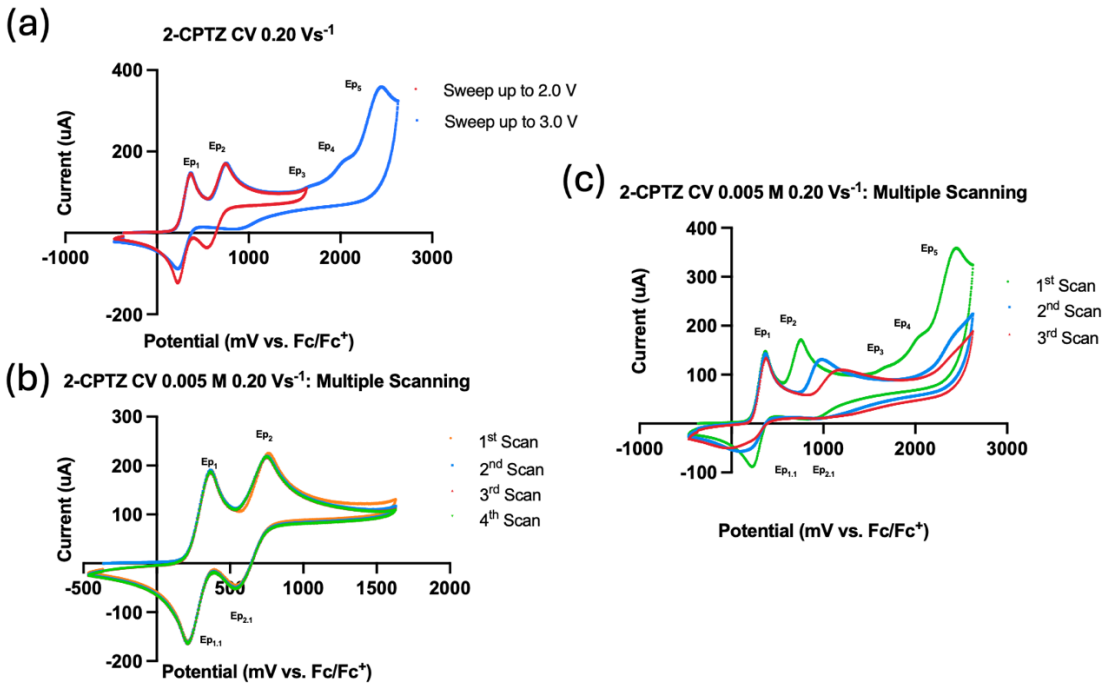

Figure 2. CV studies of 2CPTZ. a) CV studies of 2CPTZ with multiple sweeps up to 2.0 V and 3.0 V with scan rate 0.20 Vs^{-1} b) multiple scanning analysis of 2CPTZ (0.005M) sweeping up to 2.0 V c) multiple scanning analysis of 2CPTZ (0.005M) sweeping up to 3.0 V.

Figure 2(a) demonstrates than when the CV is swept up to 3.0 V, 2CPTZ undergoes five oxidation events, while only two events occur up to 1.5 V. Two first oxidation peaks (Ep_1 and Ep_2) occur at 0.376 and 0.758 V vs Fc/Fc^+, respectively. These peaks correspond to the redox species: two couple of peaks ($Ep_1/Ep_{1.1}$ and $Ep_2/Ep_{2.1}$) at a positive potential direction swept during the forward scan (anodic scan) and returning scan (cathodic scan) during the negative potential direction swept that typically indicates reversible redox processes. To confirm the reversible redox process, the CV of 2CPTZ was scanned multiple times up to 2.0 V (**Figure 2(b)**). This showed that the cyclic voltammogram overlapped in all four sweeps at $Ep_1/Ep_{1.1}$ (0.376 V/0.211 V) and $Ep_2/Ep_{2.1}$ (0.758 V/0.534 V) indicating a fully reversible process. A scan up to 3.0 V showed three additional irreversible peaks (Ep_3 1,.676, Ep_4 2.027, and Ep_5 2.453 V). **Figure 2 (c**) shows Ep_2 shifted positively from 0.758 to 0.988 to 1.176 V during the first, second, and third sweeps, respectively. Additionally, there are only two oxidation events for the two successive scans, which means the electrochemical processes occurring at the electrode surface may involve complex redox reactions, new chemical species, intermediates, or side reactions that influence the observed peaks during successive scans. A proposed electrochemical process can be tentatively inferred from these CV results (**Figure 3**).

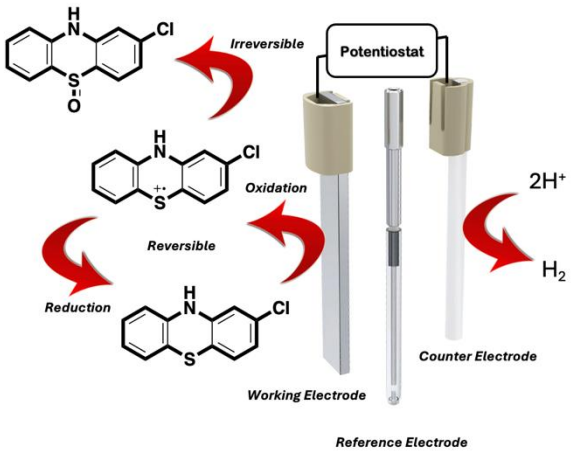

Figure 3. Proposed initial cyclic voltammetric process observed with 2-CPTZ.

Figure 4(a) revealed the scan rate effect in 2CPTZ CV studies. The selected scan rate for this study ranged from 0.05 to 0.30 Vs^{-1} with 0.05 Vs^{-1} as an incremental constant for each running cycle. **Figure 4(a)** uncovered the effect of scan rate variation on the peak current recorded for 2CPTZ oxidation. Increasing the scan rate from 0.05 to 0.30 Vs^{-1} positively shifts the Ep value from 0.342-0.393 mV. Conversely, the coefficient diffusion decreases with the increasing scan rate variation, which demonstrates that lower sweep rates are more effective in identifying a larger number of redox species.[24] However, a lower scanning rate may result in longer experimental times and possibly might miss the second oxidation peak for the two consecutive oxidation processes as the chemical species from the first oxidation may diffuse away. Additionally, a lower scan rate potentially causes issues with the signal-to-noise ratio, particularly for slow electrode reactions.

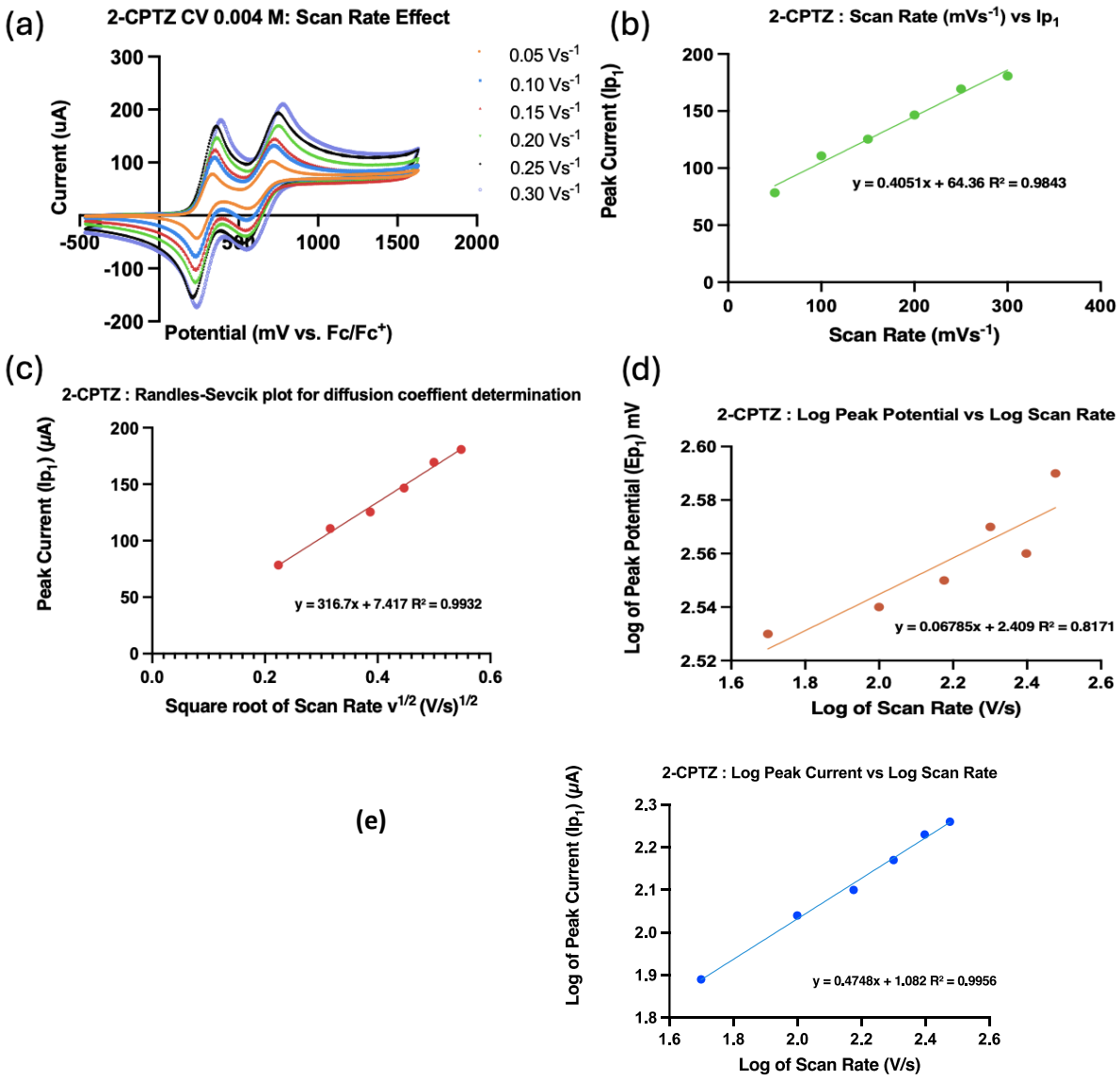

Figure 4. (a) Cyclic voltammogram of 0.004 M 2CPTZ measured at different scan rates (50-300 mVs^{-1}), (b) Plot of peak current against scan rate, (c) Randles-Sevcik plot for diffusion coefficient determination, (d) Plot of log peak potential against log scan rate, and € plot of log peak current vs log scan rate.

Scan Rate (mVs^{-1})	Anodic Peak Potential Ep_1 (mv)	Anodic Peak Current Ip_1 (µA)	Square root of Scan Rate $v^{1/2}$ $(V/s)^{1/2}$	Diffusion Coefficient (10^{-6} cm^2 s^{-1}) *
50	342	78.43	0.224	2.642
100	349	110.75	0.316	2.634
150	357	125.46	0.387	2.253
200	369	146.64	0.447	2.309
250	362	169.37	0.500	2.464
300	393	180.79	0.548	2.340

Table 2. Scan rate variations of 2CPTZ CV studies *https://www.calctool.org/physical-chemistry/randles-sevcik-equation

The effect of scan rate on 2CPTZ CV studies and the intensity of peak current was studied to determine if the redox process is controlled by diffusion or adsorption, as shown in **Figure 4(b)** and **4(c).** According to Figure **4(c),** the process can be considered diffusion controlled as the peak current is proportional to the square root of the scan rate with y= 316.7x + 7.417 R^2= 0.9932. According to **Figure 4(b)** the peak current and scan rate have a linear relationship with y= 0.4051x + 64.36 R^2= 0.9843, suggesting that the process may also be adsorption-controlled.[25] However, the process can be classified as diffusion-controlled because the plot of peak current versus the square root of the scan rate shows a higher proportional linearity relationship (R^2= 0.9932). The regression equation y= 316.7x + 7.417 with a correlation coefficient nearly to unity suggested that the 2CPTZ oxidation process over the glassy carbon electrode (GCE) surface was dominated by diffusion-controlled rather than adsorption-controlled mechanism. The study results indicate that 2CPTZ undergoes an absorption-controlled process at high scan rates rather than a diffusion-controlled process at low scan rates.[26] In this case, a slower scanning rate will allow molecules to diffuse through the bulk electrolyte towards the electrode surface, resulting in the growth of the diffusion layer. However, this event provides a certain degree of sensitivity and stability regarding peak current and peak-to-peak separation.

The relationship between these two variables can also be determined by plotting the log Ep vs Log scan rate (**Figure 4(d)**). The slope of the plot of log Ep vs log scan rate provides information about the redox process of the electrochemical reaction, including diffusion-controlled process (slope close to 0.5), adsorption-controlled process (slope close to 1.0) and mixed diffusion-adsorption process (slope between 0.5 and 1.0). Based on Figure 4 (d), the oxidation process of 2CPTZ is a diffusion-controlled process with a slope of 0.068. The slope in the anodic peak current logarithm plot (log Ip) vs the potential scan rate logarithm (log v) shows that the process is controlled by mass transfer closer to the theoretical value of 0.5 (slope: 0.47, **Figure 4(e)**).

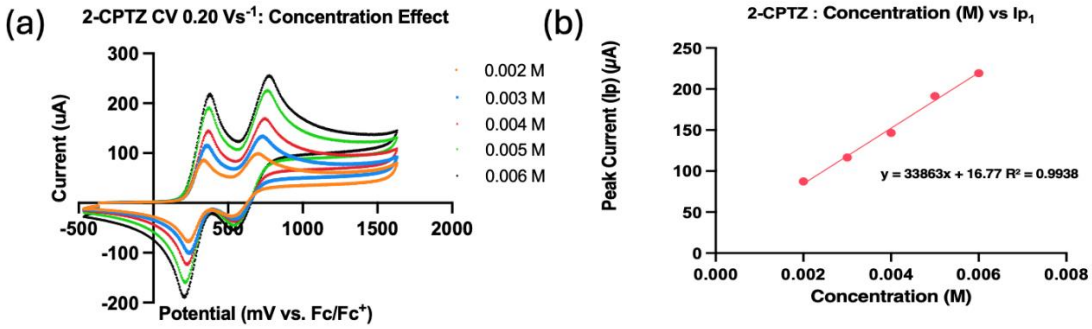

Figure 5. (a) Cyclic voltammetry measurements at various concentrations ranging from 0.002-0.006 M of 2CPTZ, (b) Calibration curve of anodic peak current against concentrations (0.002-0.006 M).

Concentration (M)	Anodic Peak Potential Ep_1 (mv)	Anodic Peak Current Ip_1 (µA)
0.002	337.09	87.31
0.003	359.07	116.58
0.004	368.77	146.61
0.005	373.69	191.41
0.006	381.04	219.21

Table 3. Concentration variations of 2CPTZ CV studies.

The Randles-Sevcik Equation was used to determine the electrochemical parameters for reversible or irreversible diffusion-controlled via a potential scan rate study. In this case, the **Eq. 1** for reversible redox process at 25 °C was used.[27-29] Where i_p is the peak current, k is a constant of 2.69 x 10^5 C/mol$\sqrt{v}$, n is the number of electrons, A is the electrode area (cm^2), D is the analytes diffusion coefficient (cm^2/s), v is the rate at which the potential is swept (V/s), and C is concentration. **Eq.2** for the irreversible redox process was also employed.[29] Where additionally, k is a constant of 2.99 x 10^5 C/mol$\sqrt{v}$ and α is the charge transfer coefficient. The charge transfer coefficient can be used to determine the number of electrons (n) involved in the irreversible oxidation process.

$$i_p = k\, n^{3/2}\, A \sqrt{Dv}\, C \qquad \textbf{Equation (1)}$$

$$i_p = kn\alpha^{1/2}\, A \sqrt{Dv}\, C \qquad \textbf{Equation (2)}$$

To investigate whether the effect of the analysis is concentration-dependent, a series of concentrations of 2CPTZ were prepared (**Table 3**). The experiment was designed to run at a scan rate of 0.20 Vs^{-1} with a step potential of 0.00244 V, sweeping from the initial and stop potential of 0 V. The step-up current responses in increasing concentration of 2CPTZ show a proportional increase in faradaic current (**Table 3**). The peak current (ip) increases with increasing analyte concentration because there are more redox-active species available to undergo oxidation at the electrode surface, and with increasing the scan rate (**Table 2**), the electrode potential changes more rapidly, and the rate of electron transfer reactions increases, leading to a larger peak current. These are consistent with the Randles-Sevcik equation and indicate the diffusion-controlled redox process.

Based on **Figures 4** and **5**, the Ep values increase as different scan rates or concentrations increase, indicating that the oxidation process depends on the difference in concentration and scan rate. The Ep depends on the scan rate or concentration if the oxidation peak potential shifts to more positive potentials. Meanwhile, the non-dependency occurs when the electrode potential remains relatively constant with increasing concentration or scan rate. The calibration curve was plotted against the concentration provided a good fitting of data that can be expressed as Ip (µA)= 33863 C + 16.77 with a correlation coefficient equal to 0.9938,

as shown in **Figure 5(b)**. The coefficient determination (R^2 value) indicates the correlation between the ip and scan rate. The closer to 0.0, the weaker the correlation between the values, and the closer to 1.0, the stronger the correlation between the values is.

Additionally, the CV of CPZ was conducted for comparison to 2-CPTZ. As shown in **Figure 6(a)**, six oxidation events were observed using a potential window up to 3.0 V. The first oxidation peak corresponds to the reversible process of redox species at an anodic potential of 0.595 V ($E_{pa}1$) and a cathodic potential of 0.492 V ($E_{pc}1$) (fast electron transfer, **Figure 6(b)**). The CV profile of CPZ is in accordance with the literature.[29] This reversible redox reaction corresponds to the oxidation of CPZ to form radical cation $CPZ^{\bullet+}$ involving a one-electron process.[30] The second to the sixth processes are irreversible behaviour and were observed at $E_{pa}1$-6: 0.765, 1.172, 1.355, 1.909, and 2.113 mV vs Fc/Fc^+, respectively. The irreversible process was confirmed swept up to 3.0 V for multiple scan analysis, indicating that after first scanning, the reaction generates new chemical species/intermediate species in the Ep_2 (**Figure 6(c)**). Ep_2 shifts to more positive potential from the first sweep 1.182 to the second sweep 1.240 V and to the third sweep 1.268 V. To determine whether the redox process during CPZ oxidation is controlled by adsorption or diffusion, a potential scan rate study was performed based on CV between 0.05 and 0.30 Vs^{-1}.

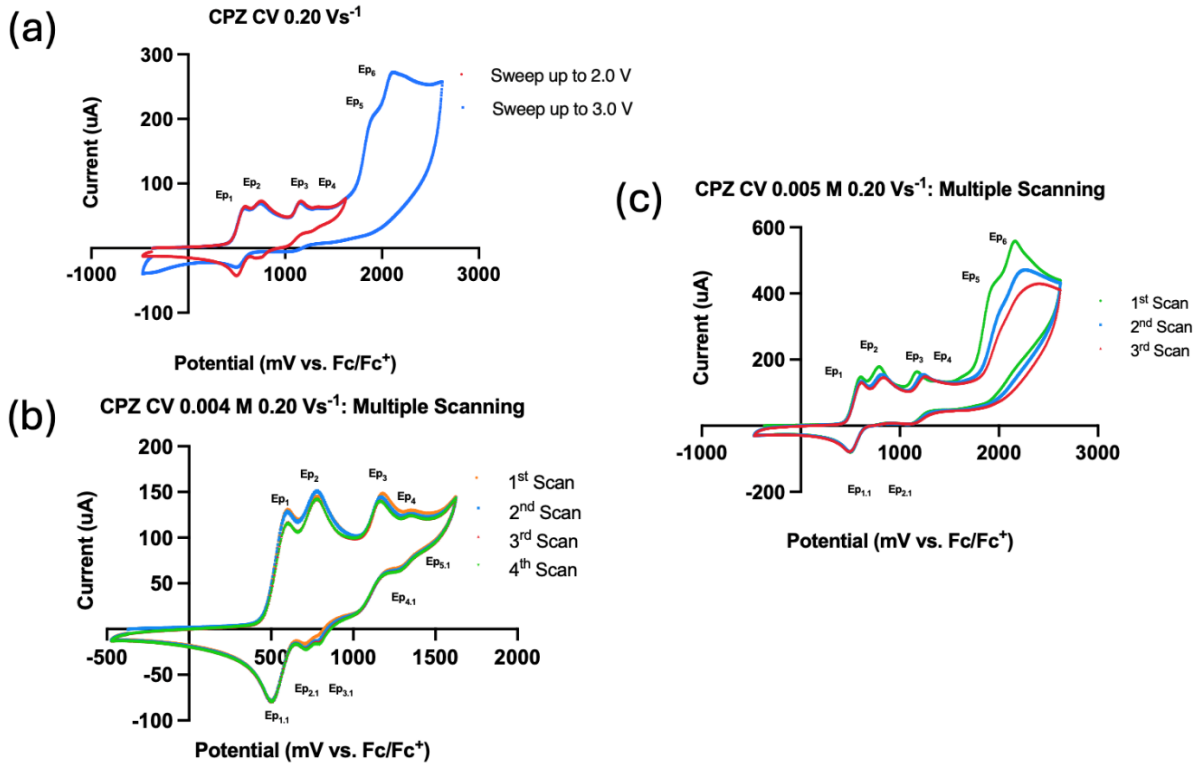

Figure 6. CV studies of CPZ. a) CV studies of CPZ with multiple sweeps up to 2.0 V and 3.0 V with scan rate 0.20 Vs^{-1} b) multiple scanning analysis of CPZ (0.005M) sweeping up to 2.0 V c) multiple scanning analysis of CPZ (0.005M) sweeping up to 3.0 V.

Based on **Figure 7** and **Table 4**, the anodic peak current plots (Ip) vs scan rate (**Figure 7(b)** and the square root of the scan rate ($v^{1/2}$) show linear trends. However, this process is dominantly controlled by diffusion with the regression equation 0.9932, **Figure 7(c)**, rather than an adsorption-controlled mechanism with regression equation 0.9305 (**Figure 7(b)**).

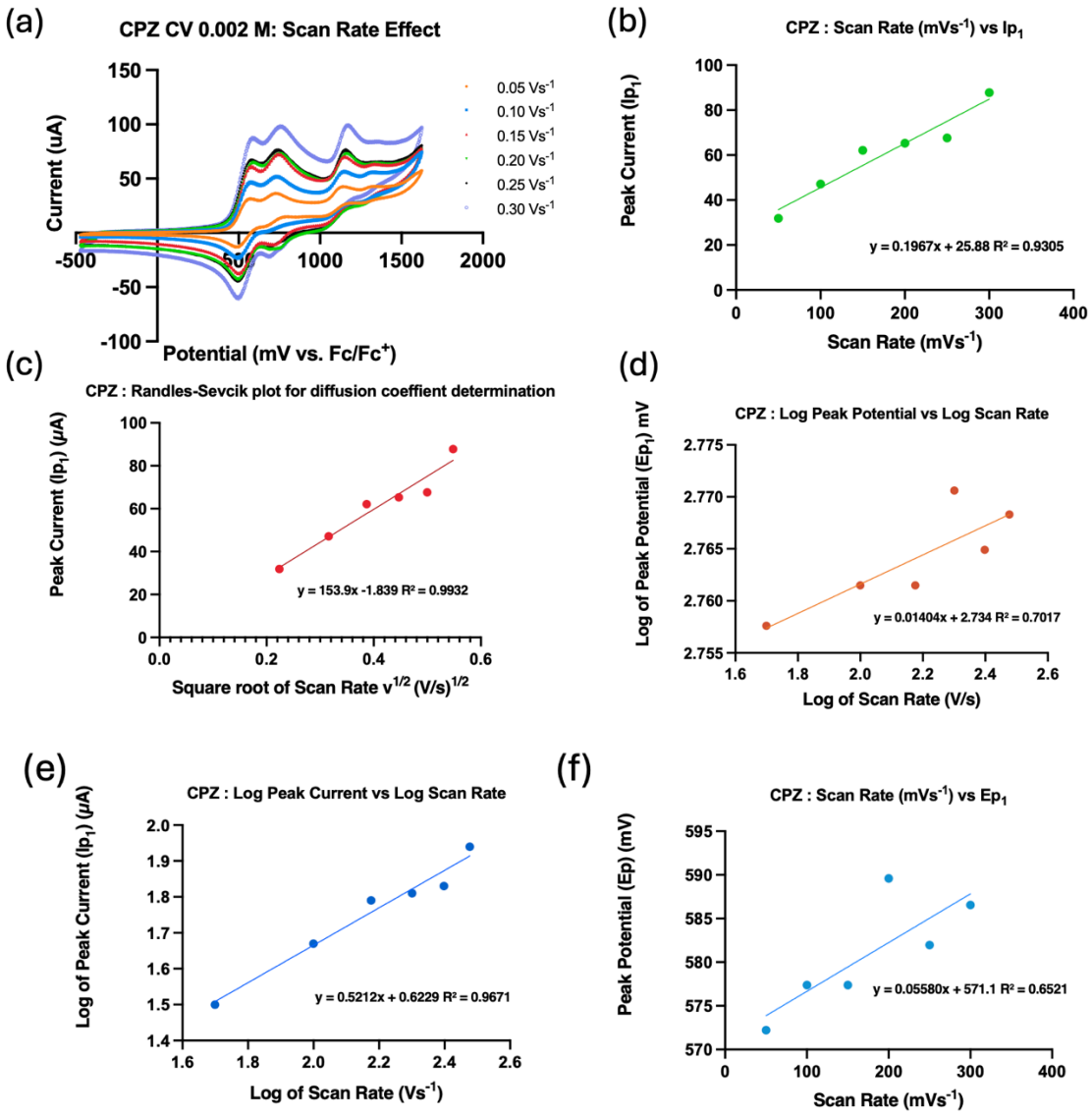

Figure 7. (a) Cyclic voltammogram of 0.002 M CPZ measured at different scan rates (50-300 mVs^{-1}), (b) Plot of peak current against scan rate, (c) Randles-Sevcik plot for diffusion coefficient determination, (d) Plot of log peak potential against log scan rate, and (e) Plot of log peak current against log scan rate, and (f) Plot of scan rate against peak potential.

Scan Rate (mVs^{-1})	Anodic Peak Potential Ep_1 (mv)	Anodic Peak Current Ip_1 (μA)	Square root of Scan Rate $v^{1/2}$ $(V/s)^{1/2}$	Diffusion Coefficient (10^{-6} cm^2 s^{-1}) *
50	572.21	31.87	0.224	1.745
100	577.39	47.15	0.316	1.910
150	577.39	62.10	0.387	2.208
200	589.60	65.31	0.447	1.832
250	581.97	67.60	0.500	1.570
300	586.55	87.80	0.548	2.207

Table 4. Scan rate variations of CPZ CV studies. *https://www.calctool.org/physical-chemistry/randles-sevcik-equation

Additionally, the slope of the plot of log Ep vs log scan rate shows that the oxidation process of CPZ is diffusion-controlled with a slope close to 0.5 (slope: 0.01404, **Figure 7(e)**); and the slope in the anodic peak current logarithm plot (log Ip) vs the potential scan rate logarithm (log v) shows that the process is controlled by mass transfer closer to the theoretical value of 0.5 (slope: 0.5212, **Figure 7(c)**).[30] In concentration and scan rate studies, CPZ shows that increasing concentrations result in an increase in peak potential. This correlation is confirmed by plotting the peak of potential against concentration (weak correlation with the regression equation 0.8896, **Figure 8(c)**) and the concentration of the analyte affects the peak current in accordance with the Randles-Sevcik equation, indicating a diffusion-controlled redox process (**Figure 8(b)** and **Table 5**. In contrast to the scan rate study, the analysis shows the non-dependent on the scan rate with the regression equation 0.6521, **Figure 7(f)**.

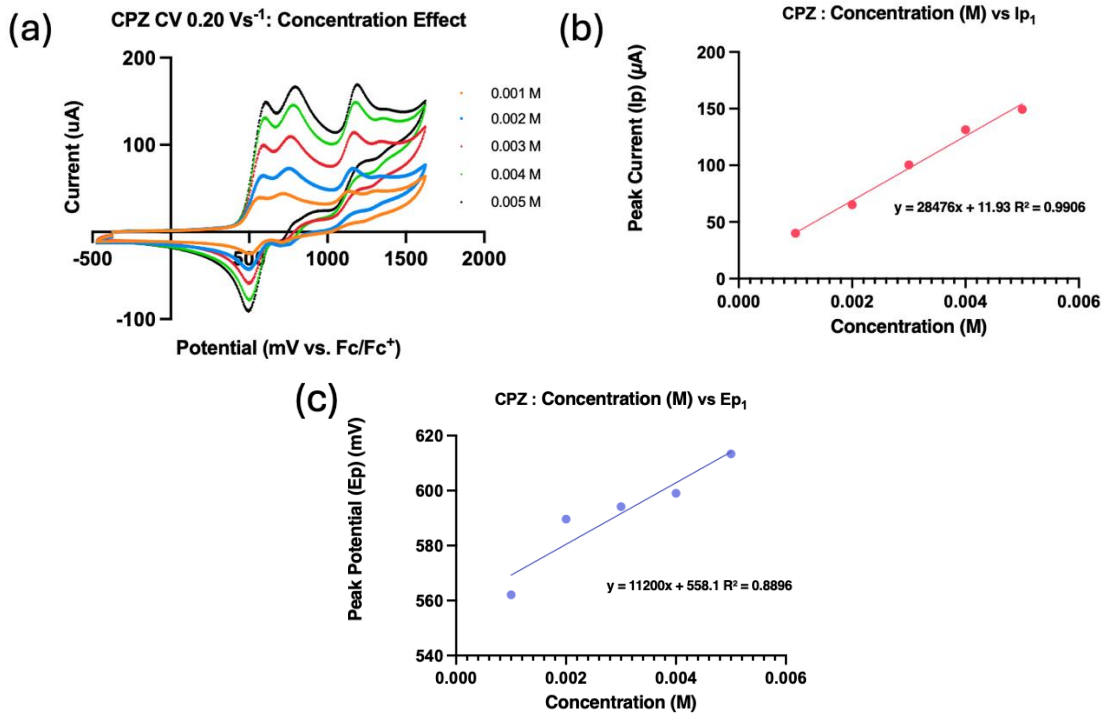

Figure 8. (a) Cyclic voltammetry measurements at various concentrations ranging from 0.001-0.005 M of CPZ, (b) Calibration curve of anodic peak current against concentrations (0.001-0.005 M), and (c) Calibration curve of anodic peak potential against concentrations (0.001-0.005 M).

Concentration (M)	Anodic Peak Potential Ep_1 (mv)	Anodic Peak Current Ip_1 (µA)
0.001	562.13	40.15
0.002	589.60	65.31
0.003	594.18	100.46
0.004	599.06	131.41
0.005	613.40	149.48

Table 5. Concentration variations of CPZ CV studies.

Optimisation of 2CPTZ metabolite electrosynthesis

In electrosynthesis, two common approaches are employed: controlled potential and controlled current. [31-32] The reaction was optimized to oxidize the compound by adjusting the desired current. To prevent the occurrence of overoxidation, a constant current of 0.5 mA to 2 mA was used for the 2CPTZ reaction. The experiment involved starting the reaction at 0.5 mA and increasing it by 0.5 mA for subsequent reactions to optimize 2CPTZ metabolite electrosynthesis. The optimisation was stopped when the current used reached the maximum applied voltage greater than 5.0 V for 24 h, and all reactions were monitored by using TLC and HPLC techniques.

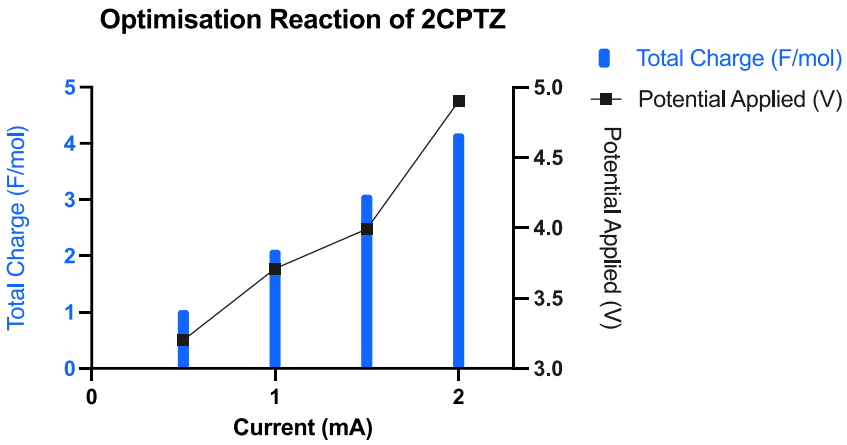

Figure 9. Constant current effect in electrosynthesis of 2CPTZ metabolites.

The starting current used for the electrosynthesis of 2CPTZ metabolites is 0.5 mA, with a maximum applied voltage of 3.2 V for 24 h. A ratio of 223:13:1 was observed for 2CPTZ, 2CPTS-SO, and 2CPTZ-SO_2, respectively. Applying a constant current of 1.0 mA (maximum applied voltage of 3.71 V), a ratio 1:16:1 for 2CPTZ, 2CPTZ-SO, and 2CPTZ-SO_2, respectively formed. Contrary to the previous condition, a constant current higher than 1.0 mA resulted in the formation of multiple unidentified oxidation metabolites (1.5 mA, 4.1 V) and mostly over-oxidised products with a constant current of 2 mA with a maximum applied voltage of 4.9 V. A summary of the optimisation and the ratio of the product are shown in **Table 6** alongside HPLC results (**Figure 10**).

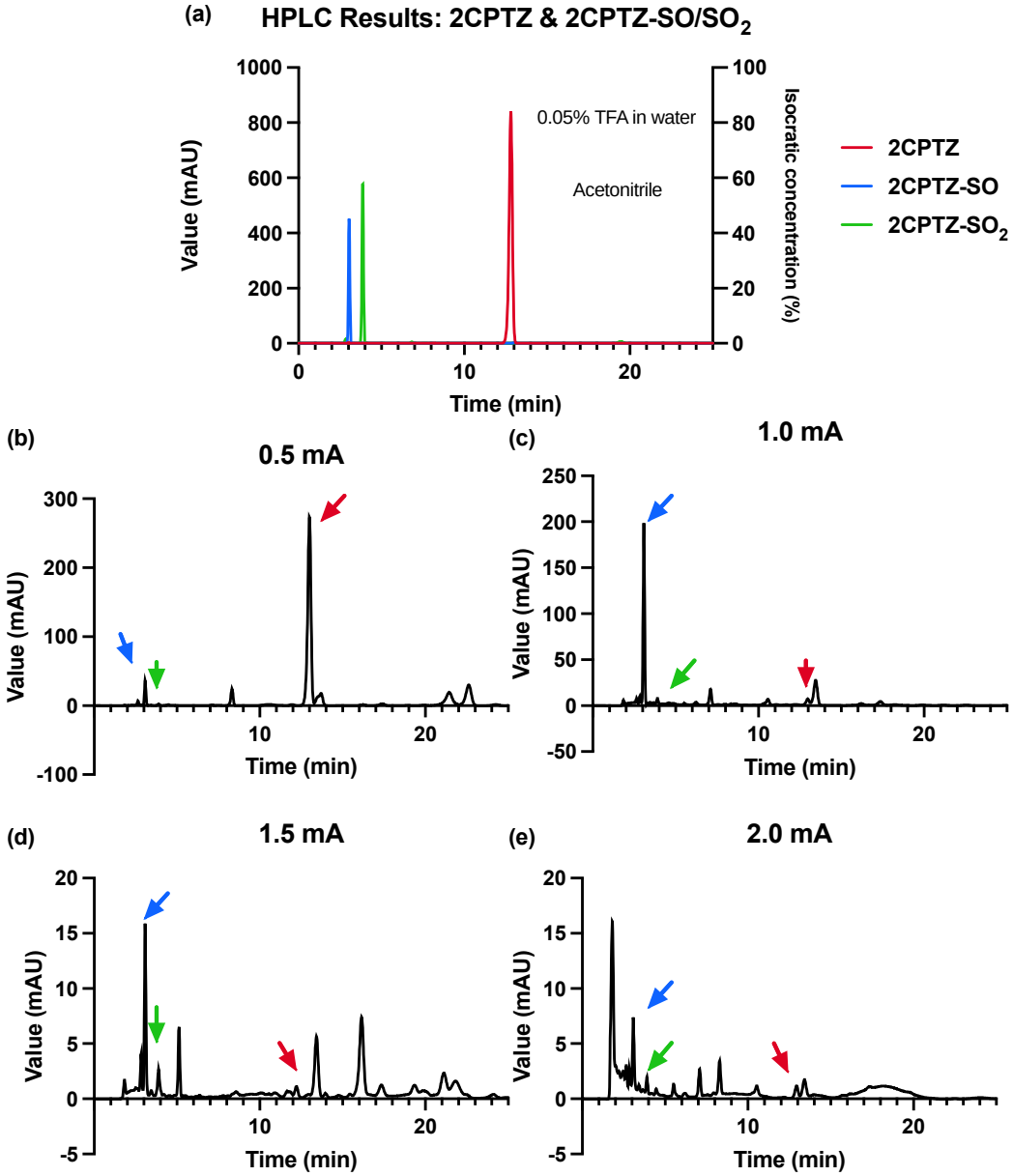

Figure 10. HPLC analysis on 2CPTZ metabolites electrosynthesis under different constant current conditions (a) HPLC of the 2CPTZ and 2CPTZ-SO/SO_2 (b) constant current of 0.5 mA, (c) constant current of 1.0 mA, (d) constant current of 1.5 mA, and (e) constant current of 2.0 mA.

Entry	Current (mA)	Max Voltage Applied (V)	Total Charged ($Fmol^{-1}$)	Ratio (HPLC Results)			Ratio of unassigned metabolites
				2CPTZ	2CPTZ-SO	2CPTZ-SO_2	
1	0.5	3.20	1.04	223	13	1	15
2	1.0	3.71	2.11	1	16	1	21
3	1.5	4.10	3.03	1	47	11	21
4	2.0	4.90	4.18	1	5	1	25

Table 6. The optimisation of 2CPTZ by using ElectraSyn 2.0, 24 hours of reaction, 25 ^{o}C.

Optimisation of CPZ metabolites electrosynthesis

Informed by the 2CPTZ optimisation study, a constant current of 1.0 mA was used as the initial current for the electrosynthesis of CPZ metabolites. Based on the previous analysis of the CV profile of CPZ, the first oxidation occurs at 590 mV, 0.2 Vs^{-1}, which is higher than 2CPTZ (369 mV, 0.2 Vs^{-1}). This means that a higher current is needed to oxidize the CPZ to generate the desired metabolite. As shown in **Figure 11**, the potential difference increases proportionally to the current following Ohm's law.

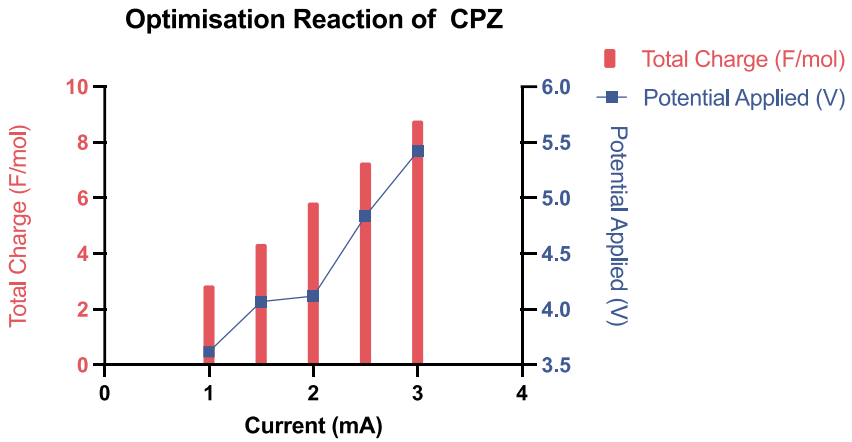

Figure 11. The constant current effect in electrosynthesis of 2CPTZ metabolites.

The optimal condition for CPZ metabolite electrosynthesis was achieved by using a constant current of 1.0 mA, maximum applied voltage of 3.86 V, with 100% CPZ conversion and generating higher specific CPZ-SO metabolite (11:1, CPZ-SO and CPZ-SO_2, respectively). Additionally, 1.0 mA was found to be the best condition due to the lowest ratio of unassigned metabolites (by HPLC and LCMS inspection). The optimisation continued to the highest current used of 3.0 mA. It can be concluded from these results that the higher the current, the more unassigned CPZ metabolites are produced, with no improvement in the ratio of the desired metabolites. **Table 7** and **Figure 12** demonstrates the optimisation table from the constant current of 1.0-3.0 mA for the CPZ metabolite reaction.

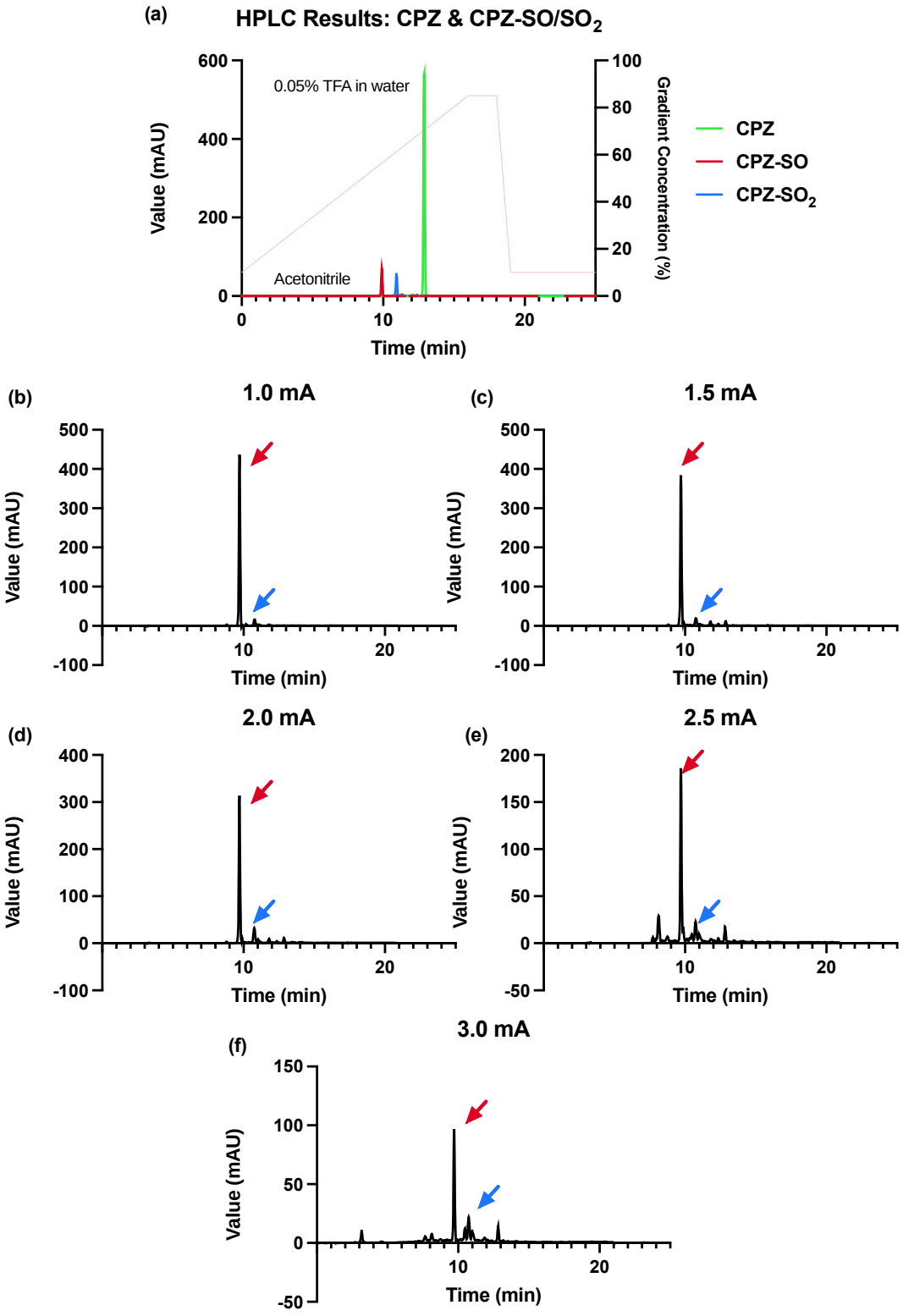

Figure 12. HPLC analysis on the CPZ metabolites electrosynthesis under different constant current conditions (a) HPLC of the 2CPTZ and 2CPTZ-SO/SO_2 (b) constant current of 0.5 mA, (c) constant current of 1.0 mA, (d) constant current of 1.5 mA, and (e) constant current of 2.0 mA.

Entry	Current (mA)	Max Voltage Applied (V)	Total Charged ($Fmol^{-1}$)	Ratio (HPLC Results)			Ratio of unassigned Metabolites
				CPZ	CPZ-SO	CPZ-SO_2	
1	1.0	3.86	2.81	n/a	11	1	5
2	1.5	4.07	4.35	1	35	3	9
3	2.0	4.12	5.84	1	25	4	12
4	2.5	4.84	7.28	1	11	2	17
5	3.0	5.09	8.61	1	7	2	20

Table 7. The optimisation of CPZ by using ElectraSyn 2.0, 24 hours of reaction, 25°C.

During the oxidation process, the reaction mixture changes from a clear solution to pink (~0.95 V) and dark green (at a higher voltage than 1.25 V). Likely due to the deprotonation and one-electron oxidation that occurred.[33] Upon completion of the reaction, a precipitate formed due to the overoxidation product being insoluble in acetonitrile.

Metabolite Analysis and Characterisation

Analytical techniques, such as ^{1}H-NMR, ^{13}C-NMR, MS, HPLC, LCMS, and IR, were employed to characterise the metabolites from the reaction. In the case of 2CPTZ, two major metabolites have been successfully isolated in their pure form, including 2CPTZ-SO (sulfoxide metabolite) and 2CPTZ-SO_2 (sulfone metabolite), for the first time (**Scheme 3**).

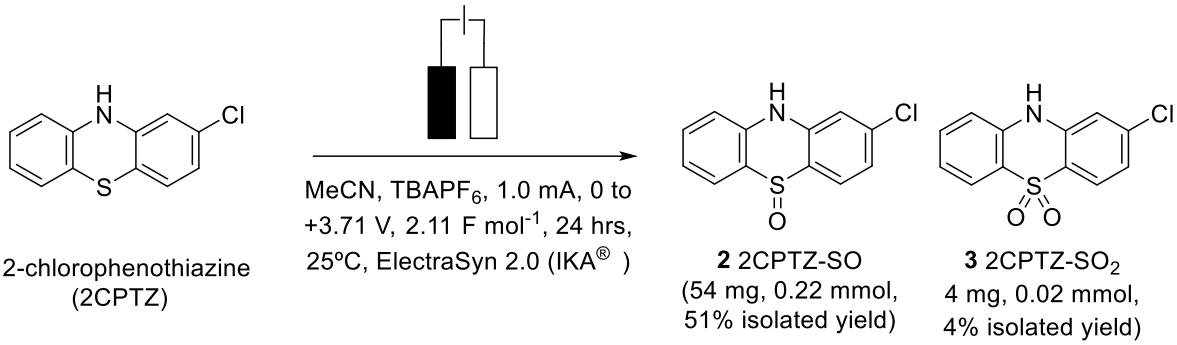

1 2-chlorophenothiazine (2CPTZ)

2 2CPTZ-SO (54 mg, 0.22 mmol, 51% isolated yield)

3 2CPTZ-SO_2 4 mg, 0.02 mmol, 4% isolated yield)

Scheme 3. Electrosynthesis of 2CPTZ metabolites, 2CPTZ-SO and 2-CPTZ-SO_2.

Purifying the metabolites involves removing $TBAPF_6$ from the crude reaction mixture through methanol recrystallization, as outlined in Procedure B (supporting information), yielding approximately 72% recovery of the crystal. The crystal was identified as $TBAPF_6$ using ^{1}H-NMR spectroscopic analysis (**Figure 13**).

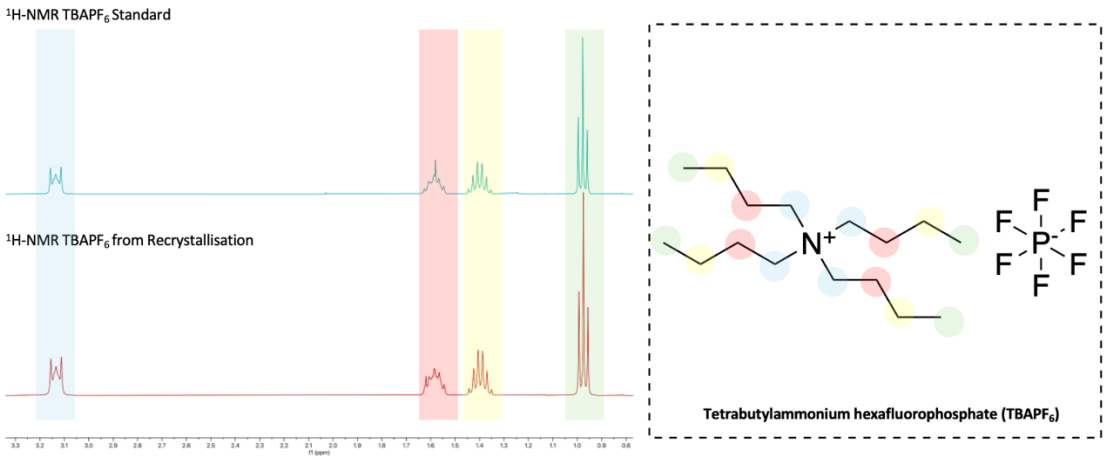

Figure 13. The stacked 400 MHz ^{1}H-NMR spectra (in $CDCl_3$) of the $TBAPF_6$ standard and from recrystallisation.

Similarly, using the optimised conditions CPZ was electro metabolized to CPZ-SO (68%) and the sulfone was detected (CPZ-SO_2) but not isolated (**Scheme 4**).

CPZ Metabolites

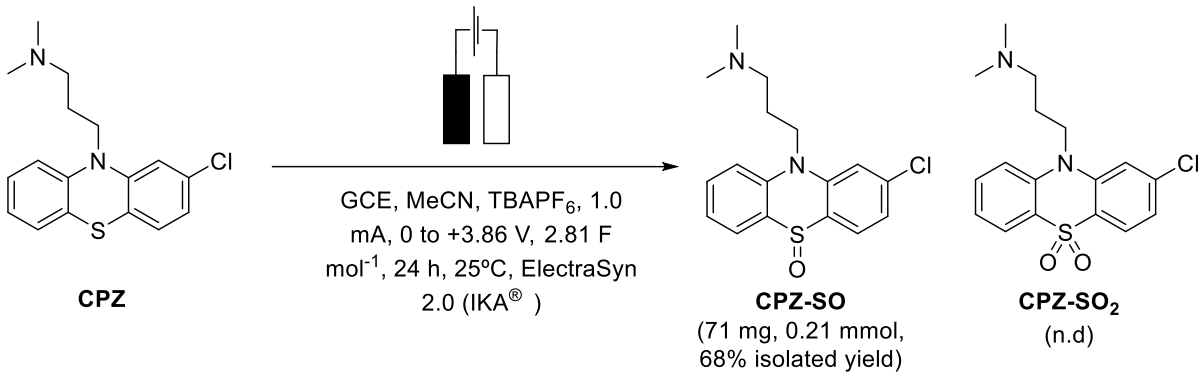

Scheme 4. Electrosynthesis of CPZ to metabolites CPZ-SO and CPZ-SO_2.

The proposed oxidation mechanism of phenothiazine derivate containing thioether (S) to form sulfoxide (SO) - sulfone (SO_2) is described below in **Scheme 5**.

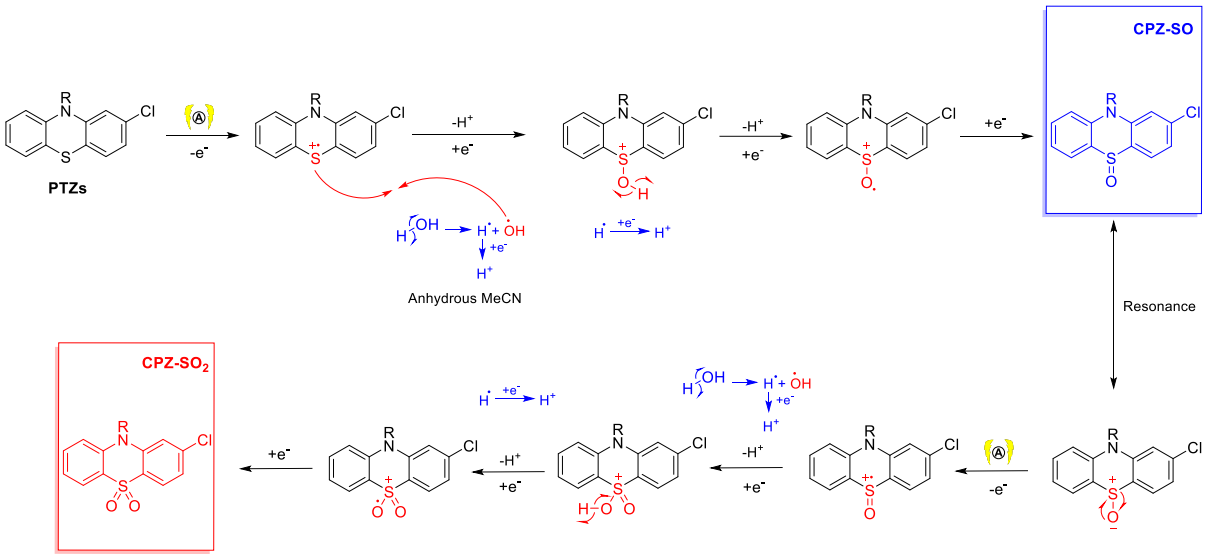

Scheme 5. A representative mechanism for the electrosynthesis of SO/SO_2 formation from PTZs.

During this study, the oxidation process occurred at the anode while the reduction process occurred at the cathode to maintain the balance of the oxidation reaction. The formation of phenothiazine sulfoxide resulted from an electrochemical reaction, where the drug underwent oxidation (loss of one electron) and formed a radical cation (step 2). The electrosynthesis reaction was carried out in a non-anhydrous MeCN solvent. During this step, water is reduced to produce hydrogen gas and hydroxide ions. The presence of hydrogen gas can be observed as bubble formation at the top of the electrochemical vial. The hydroxide ions present in the solution can attack the radical species, leading to the formation of an intermediate species in step 3. The intermediate can undergo rearrangement reactions where atoms within the molecule are reorganized to form new functional groups. This process can lead to the formation of CPZ-SO (step 4). The CPZ-SO molecule undergoes resonance in (step 5). In the case of CPZ-SO_2, forming a sulfone would require further oxidation of the

sulfoxide functional group and typically involves the addition of hydroxide ions to the sulfur atom (step 6). CPZ-sulfone is generally more stable than sulfoxide due to the presence of two oxygen atoms bonded to the sulfur atom (step 7).

In silico predictions of PTZs metabolism

Phase I metabolism of drugs usually involves chemical processes such as hydroxylation, dealkylation and oxidation to the corresponding *N*-oxide or sulfoxides.[34] Cytochromes (CYP1A2, CYP2B6, CYP2D6, CYP2C9, CYP2C19 and CYP3A4/5) are the pivotal isoenzymes involved in this metabolic event of most psychotropic drugs.[35] A study proved that CYP1A2 is the primary isoform responsible for the metabolism of CPZ (mono and di-*N*-demethylation (100%) and 5-sulfoxidation (64%) at 10 μM of CPZ. [36] Molecular docking was performed with Flare™ V 8.0.0 from Cresset using CYP1A2 (2HI4) (**Figure 14**).

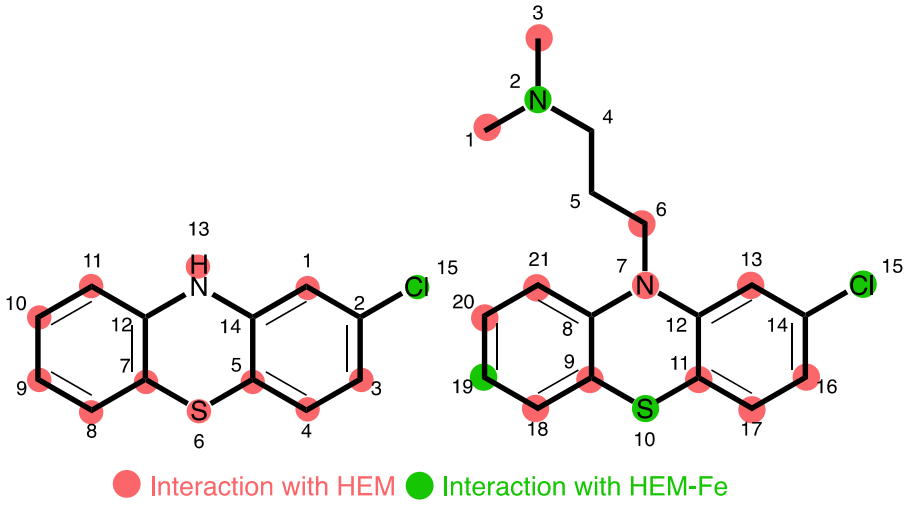

Figure 14. The Summary of PTZ Site Interaction with HEM from Docking Results

Metabolism prediction was also performed using BioTransformer 3.0 with CYP1A2, the enzyme most involved in the 2-CPTZ and CPZ metabolisms (supporting information). In addition, comprehensive studies to assess the inhibition capability of atypical antipsychotic drugs, including CPZ, levomepromazine, thioridazine, olanzapine, and risperidone in human liver microsomes have been reported. [37] This study revealed that CPZ is the only antipsychotic drug that inhibited CYP1A2 activity with IC_{50} 9.5 μM whilst levomepromazine and thioridazine (IC_{50} 3.5–25.5 μM) inhibited CYP2D6, Olanzapine (IC_{50} 14.65–42.20 μM) and risperidone (IC_{50} 20.7 μM) selectively inhibited CYP3A-catalyzed midazolam 1' and 4'-hydroxylation reaction.

Conclusions

In this study, we have comprehensively studied the electrochemical behaviour of a series of PTZ derivatives. Analysis of the cyclic voltammetry behaviour of PTZ derivatives revealed a SeAR based on scaffold characteristics and their respective influence on oxidation potential. Molecular modelling enabled the predicted of the most likely metabolites to form. Ultimately, an optimised electrochemical reaction platform for the parent scaffold and exemplar drug molecule enabling a tractable synthesis of the *S*-oxide and for the first time the *S*,*S*-dioxide metabolites.

Acknowledgments and Funding

R.A. gratefully acknowledges the PhD scholarship of The Center for Education Funding Services (BPI); Ministry of Education, Culture, Research, and Technology; and the Indonesia Endowment Fund for Education (LPDP), Ministry of Finance, The Republic of Indonesia. A.E.M. gratefully acknowledge the Bolashak Scholarship Program of the Ministry of Science and Higher Education, the Republic of Kazakhstan.

References

[1] Ohlow MJ, Moosmann B. Phenothiazine: the seven lives of pharmacology's first lead structure. Drug Discov Today. 2011;16(3-4):119-131. doi:10.1016/J.DRUDIS.2011.01.001

[2] Jaszczyszyn A, Gąsiorowski K, Świątek P, et al. Chemical structure of phenothiazines and their biological activity. Pharmacological Reports. 2012;64(1):16-23. doi:10.1016/S1734-1140(12)70726-0

[3] Dougherty MM, Marraffa JM. Phenothiazines. In: Encyclopedia of Toxicology: Third Edition. Elsevier; 2014:881-883. doi:10.1016/B978-0-12-386454-3.00769-7

[4] Edinoff AN, Armistead G, Rosa CA, et al. Phenothiazines and their Evolving Roles in Clinical Practice: A Narrative Review. Health Psychol Res. 2022;10(4):2022. doi:10.52965/001C.38930

[5] Dougherty MM, Marraffa JM. Phenothiazines. Encyclopedia of Toxicology: Third Edition. Published online January 1, 2014:881-883. doi:10.1016/B978-0-12-386454-3.00769-7

[6] Dahl SG. Active metabolites of phenothiazine drugs. Clinical Pharmacology in Psychiatry. Published online 1981:125-137. doi:10.1007/978-1-349-05929-4_10

[7] Bosch E. Catalytic oxidation of chlorpromazine and related phenothiazines. Cation radicals as the reactive intermediates in sulfoxide formation. Perkin transactions I /. 1995;(8):1057-1064.

[8] Wen B, Zhou M. Metabolic activation of the phenothiazine antipsychotics chlorpromazine and thioridazine to electrophilic iminoquinone species in human liver microsomes and recombinant P450s. Chem Biol Interact. 2009;181(2):220-226. doi:10.1016/J.CBI.2009.05.014

[9] Dasgupta A, Dastidar SG, Shirataki Y, Motohashi N. Antibacterial Activity of Artificial Phenothiazines and Isoflavones from Plants BT - Bioactive Heterocycles VI: Flavonoids and Anthocyanins in Plants, and Latest Bioactive Heterocycles I. In: Motohashi N, ed. Springer Berlin Heidelberg; 2008:67-132. doi:10.1007/7081_2007_108

[10] Wang J, Xu R, Xu A. Solubility determination and thermodynamic functions of 2-chlorophenothiazine in nine organic solvents from T = 283.15 K to T = 318.15 K and mixing properties of solutions. J Chem Thermodyn. 2017;106:132-144. doi:10.1016/J.JCT.2016.11.029

[11] Moran NC, Butler WM. THE PHARMACOLOGICAL PROPERTIES OF CHLORPROMAZINE SULFOXIDE, A MAJOR METABOLITE OF CHLORPROMAZINE. A COMPARISON WITH CHLORPROMAZINE. Journal of Pharmacology and Experimental Therapeutics. 1956;118(3).

[12] Yeung PKF, Hubbard JW, Korchinski ED, Midha KK. Pharmacokinetics of chlorpromazine and key metabolites. Eur J Clin Pharmacol. 1993;45(6):563-569. doi:10.1007/BF00315316

[13] Jaworski TJ, Hawes EM, Mckay G, Midha KK. The metabolism of chlorpromazine n-oxide in man and dog. Xenobiotica. 1990;20(1):107-115. doi:10.3109/00498259009046817

[14] Owens ML, Juenge EC, Poklis A. Convenient oxidation of phenothiazine salts to their sulfoxides with aqueous nitrous acid. J Pharm Sci. 1989;78(4):334-336. doi:10.1002/JPS.2600780415

[15] Noyori R, Aoki M, Sato K. Green oxidation with aqueous hydrogen peroxide. doi:10.1039/b303160h

[16] Liu K, Meng J, Jiang X. Gram-Scale Synthesis of Sulfoxides via Oxygen Enabled by Fe(NO3)3·9H2O. Org Process Res Dev. 2023;27(7):1198-1202. doi:10.1021/ACS.OPRD.2C00390/SUPPL_FILE/OP2C00390_SI_003.PDF

[17] Stalder R, Roth GP. Preparative microfluidic electrosynthesis of drug metabolites. ACS Med Chem Lett. 2013;4(11):1119-1123. doi:10.1021/ML400316P

[18] Asra, R., Jones, A. M. “Green electrosynthesis of drug metabolites” Toxicol. Res. 2023, 12(2), 150-177 https://academic.oup.com/toxres/article/12/2/150/7071047

[19] Fuchigami, H., Bal, M. K., Brownson, D. A. C., Banks, C. E., Jones, A. M. “Voltammetric behaviour of drug molecules as a predictor of metabolic liabilities” Scientia Pharmaceutica, 2020, 88, 46. https://www.mdpi.com/2218-0532/88/4/46

[20] Wetzel, A., Jones, A. M. “Electrically-driven N(sp2)-C(sp2/3) bond cleavage of sulfonamides” ACS Sustain. Chem. Eng. 2020 8, 3487-3493. https://pubs.acs.org/doi/full/10.1021/acssuschemeng.0c00387

[21] Bal, M. K., Banks, C. E., Jones, A. M. “Metabolism mimicry: An electrosynthetic method for the selective deethylation of tertiary benzamides” ChemElectroChem 2019, 6, 4284-4291. ICS paper of the month (Feb 2019) https://chemistry-europe.onlinelibrary.wiley.com/doi/abs/10.1002/celc.201900028

[22] Asra, R., Povinelli, A.P.R., Zazeri, G., Jones, A.M. Computational Predictive and Electrochemical Detection of Metabolites (CP-EDM) of Piperine, 2024, ChemRxiv, 2024, 10.26434/chemrxiv-2024-4lt9w

[23] Chooto P, Chooto P. Cyclic Voltammetry and Its Applications. Voltammetry. Published online January 28, 2019. doi:10.5772/INTECHOPEN.83451

[24] Teli AM, Bhat TS, Beknalkar SA, et al. Bismuth manganese oxide based electrodes for asymmetric coin cell supercapacitor. Chemical Engineering Journal. 2022;430:133138. doi:10.1016/J.CEJ.2021.133138

[25] Yusoff F, Aziz A, Mohamed N, Ab Ghani S. Synthesis and Characterizations of BSCF at Different pH as Future Cathode Materials for Fuel Cell. Int J Electrochem Sci. 2013;8(8):10672-10687. doi:10.1016/S1452-3981(23)13139-7

[26] Tukimin N, Abdullah J, Sulaiman Y. Development of a PrGO-Modified Electrode for Uric Acid Determination in the Presence of Ascorbic Acid by an Electrochemical Technique. Sensors 2017, Vol 17, Page 1539. 2017;17(7):1539. doi:10.3390/S17071539

[27] Aljabali AAA, Barclay JE, Butt JN, Lomonossoff GP, Evans DJ. Redox-active ferrocene-modified Cowpea mosaic virus nanoparticles. Dalton Transactions. 2010;39(32):7569. doi:10.1039/c0dt00495b

[28] Bard A, ’Faulkner L. Electrochemical Methods: Fundamentals and Applications, 2nd Edition. 2nd ed. John Wiley & Sons, Inc.; 2000.

[29] Martinez-Rojas F, Espinosa-Bustos C, Ramirez G, Armijo F. Electrochemical oxidation of chlorpromazine, characterisation of products by mass spectroscopy and determination in pharmaceutical samples. Electrochim Acta. 2023;443:141873. doi:10.1016/J.ELECTACTA.2023.141873

[30] Takamura K, Inoue S, Kusu F, Otagir M, Uekama K. Electrochemical Oxidation of Chlorpromazine-Cyclodextrin Inclusion Complex. Chem Pharm Bull (Tokyo). 1984;32(3):839-845. doi:10.1248/CPB.32.839

[31] Rahman MH, Bal MK, Jones AM. Metabolism-Inspired Electrosynthesis. ChemElectroChem. 2019;6(16):4093-4104. doi:10.1002/celc.201900117

[32] Schotten C, Nicholls TP, Bourne RA, Kapur N, Nguyen BN, Willans CE. Green Chemistry TUTORIAL REVIEW Making electrochemistry easily accessible to the synthetic chemist. Published online 2020. doi:10.1039/d0gc01247e

[33] Sigmund LM, Ebner F, Jöst C, et al. An Air-Stable, Neutral Phenothiazinyl Radical with Substantial Radical Stabilization Energy. Chemistry. 2020;26(14):3152. doi:10.1002/CHEM.201905238

[34] Krämer M, Broecker S, Madea B, Hess C. Confirmation of metabolites of the neuroleptic drug prothipendyl using human liver microsomes, specific CYP enzymes and authentic forensic samples—Benefit for routine drug testing. J Pharm Biomed Anal. 2017;145:517-524. doi:10.1016/J.JPBA.2017.07.011

[35] Zhou SF, Liu JP, Chowbay B. Polymorphism of human cytochrome P450 enzymes and its clinical impact. Drug Metab Rev. 2009;41(2):89-295. doi:10.1080/03602530902843483

[36] Wójcikowski J, Boksa J, Daniel WA. Main contribution of the cytochrome P450 isoenzyme 1A2 (CYP1A2) to N-demethylation and 5-sulfoxidation of the phenothiazine neuroleptic chlorpromazine in human liver—A comparison with other phenothiazines. Biochem Pharmacol. 2010;80(8):1252-1259. doi:10.1016/J.BCP.2010.06.045

[37] Gervasini G, Caballero MJ, Carrillo JA, Benitez J. Comparative Cytochrome P450 In Vitro Inhibition by Atypical Antipsychotic Drugs . ISRN Pharmacol. 2013;2013:1-5. doi:10.1155/2013/792456